Journal of Clinical and Medical Images

Research Article ISSN 2640-9615 |Volume 6

Utilization of the A/T Ratio on Ultrasound and A Clinical Model to Diagnose Malignant Thyroid Nodules

Chao Zhou[1#], Chaoli Xu[2*#], Bin Yang[2*], Zheng Zhu[1*], Yan Huang[1], Bo Shen[1], Xueming Dong[1], Xinyan Xu[1] and Guotao Liu[1]

[1]Department of Ultrasound Diagnostic, The First People's Hospital of Taicang, Taicang 215400, P. R. China

[2]Department of Ultrasound Diagnostic, Jinling Hospital, School of Medicine, Nanjing University, Nanjing 210002, P. R. China

#These authors contributed equally.

***Corresponding author:**

Xu Chaoli,
Department of Ultrasound Diagnostic, Jinling Hospital, School of Medicine, Nanjing University, Nanjing 210002, P. R. China,
Tel: +86-15751866703,
E-mail: 15751866703@163.com

Yang Bin,
Department of Ultrasound Diagnostic, Jinling Hospital, School of Medicine, Nanjing University, Nanjing, 210002, P. R. China,
Tel: +86-13951749052,
E-mail: yangbin12yx@163.com

Zhu Zheng,
Department of Ultrasound Diagnostic, The First People's Hospital of Taicang, Changsheng South Road, Taicang 215400, P. R. China,
Tel: +86-18915768091,
E-mail: zhuzheng751213@163.com

Received: 21 Jan 2022
Accepted: 31 Jan 2022
Published: 05 Feb 2022
J Short Name: JCMI

Citation:

Xu Chaoli and Yang Bin and Zhu Zheng, Utilization of the A/T Ratio on Ultrasound and A Clinical Model to Diagnose Malignant Thyroid Nodules. J Clin Med Img. 2022; V6(3): 1-8

#Author Contributions:

Chao Zhou, Chaoli Xu, thse authors are contributed equally to this article

1. Abstract

1.1. Background: To identify the Anteroposterior/Transverse diameter (A/T) ratio on Ultrasound (US) and use a clinical model to discriminate between benign and malignant thyroid nodules.

1.2. Methods: A total of 1,218 thyroid nodules (training dataset) and 601 thyroid nodules (validation dataset) were enrolled. Clinical and US features were extracted for a random forest model and to estimate the weight of each feature. Subsequently, a nomogram model was constructed for external validation. Finally, the diagnostic performances of the models were determined.

1.3. Results: The Area Under the Curve (AUC) of the random forest model showed good discrimination in the training dataset and validation dataset (AUC: 0.897 vs. 0.769), which was significantly higher than that without the A/T ratio in the models (AUC: 0.862 vs. 0.716) (all P<0.05). The nomogram model based on the top three significant highest risk factors (A/T ratio, age, and multiple microcalcifications) showed an AUC of 0.818 in the validation dataset, which was also significantly higher than that without the A/T ratio in the model (AUC 0.732) (P<0.05). The AUC of the A/T ratio as a single feature in the training dataset was 0.735, with a cutoff value of nearly 0.9 and a specificity of 95%, which yielded an AUC of 0.745, sensitivity of 74.81%, and specificity of 85.29% for diagnosing malignancy in validation dataset.

1.4. Conclusion: The clinical and US feature-derived clinical model had a good performance for diagnosing thyroid malignancy, while an A/T ratio≥0.9 can reduce misdiagnosis and add more contribution for diagnostic performance.

2. Introduction

Thyroid nodules are commonly seen in clinical practice, with an estimated prevalence ranging from 25 to 70% in adults, and over 10% of these nodules are malignant with the use of Ultrasound (US) [1, 2]. Several guidelines have been published to provide an easy-to-use US-based method to classify thyroid nodules, reduce unnecessary biopsies, detect thyroid malignancies that are likely to cause patient harm and thus avoid misdiagnosis as well as overtreatment [3-5]. Accordingly, the US features of malignant thy-

roid nodules, including microcalcifications, a solid composition, anteroposterior to transverse diameter ratio (A/T) ≥1, markedly hypoechoic echotexture, and irregular margins, have been well characterized. [6-9] Notably, studies have shown that nodules with an A/T≥1 have an 8.6- to 25.3-fold higher risk of being malignant than nodules with other characteristics [10, 11], yielding a relatively high specificity ranging from 60.0% to 100.0% [7-16]. However, there remains an evidence gap regarding the diagnosis of thyroid cancer using A/T≥1. For example, the prevalence of incidental A/T≥1 found in malignancies was only 44-68%, and a "gray zone" still exists, with approximately 32-56% of the A/T ratio<1 remaining malignancy or indeterminate after stratification even after fine-needle biopsy [7, 8, 10, 17]. Given these results, further workup with an exact or specific diagnostic cutoff point of the A/T ratio to distinguish between benign and malignant nodules and reduce the misdiagnosis is highly desirable.

Several studies have proposed that A/T >1.2 improves the specificity for malignant risk assessment [15, 18, 19], although these studies are invariably one-sided and lack reproducibility due to their heterogeneity and insufficient patient data. These considerations suggested that a slightly higher A/T ratio threshold for nodules might improve the specificity of risk stratification systems in ruling out malignancy and might deteriorate the detection rate in pinpointing nodules for biopsy. Furthermore, in those studies, US findings and tumor clinicopathologic characteristics were simultaneously incorporated to predict malignancy [11, 19, 20], or a risk model was developed for predicting malignancy in a subgroup of patients [21-23]. Considering that US characteristics, such as size, morphology, and position, might be directly related to the probability of malignancy, it is necessary to explore the independent contributions of thyroid lesion US features, especially the A/T ratio, in determining the likelihood of malignancy in a preoperative patient population.

In recent years, machine learning algorithm-based clinical models have attracted much attention in precise imaging-based diagnosis and prediction with AUCs from 0.808 to 0.904 [24, 25] when compared to those in clinical practice with AUCs from 0.551 to 0.678 [11, 19-23], verifying that the combination of US features of primary tumors and machine learning may yield a great diagnostic effect for predicting thyroid malignancies, owing to its advantages of being fast, accurate, reproducible, and applicable to other outcomes [26-28]. However, until now, a machine learning-based clinical model for the A/T ratio for thyroid malignancy with US has not yet been devised. Therefore, it is necessary to explore its independent contribution to determining the likelihood of malignancy for the patient population in a preoperative setting.

The aim of this study was to use a machine learning algorithm to construct a clinical model with US to predict malignancy and determine an independent specific cutoff point for the A/T ratio in clinical practice, which could be feasible for only an A/T ratio of sonographic criteria for identifying nodal malignant preoperatively or recommending fine-needle biopsy in thyroid nodules and increasing the thyroid cancer detection rate independent of the size.

3. Materials and Method

3.1. Patients

A total of 949 patients with 1,218 thyroid lesions were enrolled consecutively for the training dataset from January 2014 to December 2020 in Jinling Hospital. We also obtained data from 547 patients with 601 lesions for the validation dataset at the First People's Hospital of Taicang. The clinical data, US images, and pathological results were retrospectively reviewed. The inclusion criteria were as follows: (1) pathological diagnosis of malignant thyroid nodules and pathological confirmation as benign nodules that have suspicious features on US images for malignancy; (2) US scan of the thyroid acquired within one month before surgery; (3) pathologically identified lesions with a diameter equal to or less than 3 cm; and (4) preoperative location and labeling by a US radiologist with more than 10 years of experience. All matched lesions were sent for pathologic examination. The exclusion criteria were as follows: (1) biopsy performed before US scanning; (2) target neoplasms that could not be visualized on US; and (3) incomplete clinical and pathological information. This study was approved by the institutional review board of Jinling Hospital and the First People's Hospital of Taicang and informed consent was obtained.

3.2. US Scanning and Imaging Acquisition

All of the included patients underwent US scanning before surgery. High-quality US images were acquired with commercial US devices (IU22 (Philips), Logic9 (GE)) with linear probes (3-12 MHz, centered at 10 MHz). Before collecting US data, all US radiologists involved in the acquisition of US images had more than 5 years of experience in thyroid US. They underwent rigorous training to standardize the imaging parameter adjustment method and the US scanning procedure of the thyroid according to the AIUM practice guideline for performing thyroid US [29]. It is routinely required to acquire images of the anteroposterior and transverse sections of the target nodules for subsequent analysis. To avoid bias in the measurements, nodules larger than 3 cm displayed on the images were excluded. All the data of each sub center were gathered and reviewed for further analysis by two senior US radiologists blinded to the clinical and pathological results, and only the data that passed the quality control examination were included.

3.3. Feature Extraction

The variables used for model development included both clinical and image features. The clinical variables included sex, age, and the serum Thyroid-Stimulating Hormone (TSH), Triiodothyronine (T3), Free Triiodothyronine (FT3), Thyroxine (T4), and Free Thyroxine (FT4) levels, and the imaging variables included thyroid size and nodule size, the A/T ratio, position of the nodule, loca-

tion within the lobe, nodule morphology, nodule boundary, nodule margin, echogenicity, posterior echo attenuation, side shadowing, halo, lesion calcification and blood flow. These features were extracted and used to estimate the probability of malignancy (detailed in Table S1). Two radiologists read the images and performed feature extraction. The missing data rates of all features were less than 10%. Regarding missing data, mean interpolation was used for continuous variables, and mode interpolation was used for rank or classification variables. The class variables were then coded with features, and 53 features were obtained.

Statistical analysis was performed using the SPSS 22.0 software package (SPSS, Chicago, IL, USA) and R (http://www.R-project.org). Continuous variables were compared using the paired Student's t test or Mann-Whitney U-test, while discrete variables were compared using the chi-square or Fisher's exact test, as appropriate. Only statistically significant variables (P<0.05) from univariable analysis were entered into the multivariable analysis to evaluate the association between malignancy and the risk factors. We also performed variance analysis for the features. The sequential method of Bonferroni correction was applied to adjust the baseline significance level ($\alpha = 0.05$) for multiple testing bias. A p-value < 0.05 was considered statistically significant.

3.4. Model Construction and Validation

First, the random forest algorithm was used to build the classifier model and evaluate all of the features for their ability to predict benign and malignant thyroid nodules. Then, the weighted features were screened out according to their respective coefficients. The feature selection process used the least absolute shrinkage and selection operator algorithm with a penalty term called L1-norm (C-index was set as 1.00). Finally, the models were constructed using 5-fold cross-validation in the training dataset and were tested independently in the validation dataset. Calibration curves were plotted to assess the calibration of the random forest models, accompanied by the Hosmer-Lemeshow test. (A significant result implies that the model does not calibrate perfectly.) Decision curve analysis was conducted to determine the clinical usefulness of the model by quantifying the net benefits at different threshold probabilities in the validation dataset.

Second, to provide clinicians with a quantitative tool to predict the individual probability of malignancy, a nomogram based on the risk predictive factors obtained by multivariate logistic regression analyses was built. To choose the most significant parameters for predicting malignancy, we chose the top 3 parameters associated with the highest risk. The model was constructed in the training dataset and tested independently in the validation dataset. The nomogram was plotted using R with the "Hmisc" package.

Finally, we specifically evaluated the diagnostic performance of the A/T ratio as a single feature and determined a cutoff point for the A/T ratio with a high specificity of 95%. Furthermore, to evaluate the contribution of the A/T ratio to the predictive performance of the models, the A/T ratio was excluded in each model to test their predictive performance.

The diagnostic performance of each model was evaluated by using Receiver Operating Characteristic (ROC) curves and the corresponding Areas Under the Curve (AUCs). The differences between AUCs were compared using Delong analysis. The optimal cutoff value, accuracy, sensitivity, specificity, positive predictive value, and negative predictive value were calculated to assess the discriminative ability of each model.

4. Results

4.1. Clinical and Sonographic Characteristics in the Training Dataset

The training dataset consisted of 468 men and 750 women, with 288 (23.65%) lesions diagnosed as benign and 930 (76.35%) lesions diagnosed as malignant (Table S2). There were statistically significant differences in sex and age between the patients with benign and malignant nodules (Table S3). More female patients (50.08%) had malignant nodules (P< 0.05), and the patients with malignant nodules were younger than those without malignant nodules (49.65±11.18 years vs. 42.81±12.02 years, P< 0.05). However, there were no significant differences in FT3, FT4, TSH, T3, and T4 values between the two groups.

According to the Mann-Whitney U test and chi-square or Fisher's exact test, malignant tumors had a higher A/T ratio than benign lesions (0.89±0.27 vs. 0.69±0.19, P=0.000) and were more likely to have markedly irregular morphology (46.45% vs. 13.54%, P=0.000), poorly defined margins (57.74% vs. 17.01%, P=0.000), and coexisting calcifications (44.01% vs. 4.93%, P=0.000). The other characteristics of thyroid nodules, including anteroposterior diameter, boundary, echogenicity, posterior echo attenuation, side shadowing, and blood flow, were significantly different between benign and malignant nodules (P< 0.05). There were no differences in thyroid size or echogenicity between the benign and malignant groups (P > 0.05) (Table S3).

Multiple logistic regression analysis showed that the A/T ratio, multiple microcalcifications, and age were the top 3 parameters associated with the highest risk in the training dataset. The A/T ratio had a significant and positive relationship with the risk of thyroid malignancy (OR 41.833, 95% CI 14.622-119.684) (Table 1). Additionally, younger age (OR 0.961, 95% CI 0.946-0.976) and the coexistence of multiple microcalcifications (OR 4.618, 95% CI 1.032-20.671) were also independently associated with an increased risk for malignant nodules. The other parameters related to malignancy are shown in Table S4.

Table 1: The multiple regression model for the most important clinical and US characteristics of thyroid nodules in the training and validation datasets

Parameters	Training dataset						Validation dataset					
	B	SE	Wald	OR	95% CI	*P*	B	SE	Wald	OR	95% CI	*P*
A/T ratio	3.734	0.536	48.465	41.833	14.622-119.684	0	3.23	1.421	5.164	25.285	1.559-410.054	0
Age	-1.204	0.008	24.476	0.961	0.946-0.976	0	-0.007	0.012	32.984	0.932	0.910-0.955	0
Calcification (multiple microcalcifications)	1.53	0.765	4.004	4.618	1.032-20.671	0.045	1.091	0.5	4.764	2.976	1.118-7.924	0.029

SE: standard error; OR: odds ratio; CI: confidence interval.

4.2. Clinical and Sonographic Characteristics in the Validation Dataset

The validation dataset consisted of 171 (28.45%) lesions diagnosed as benign and 430 (71.55%) lesions diagnosed as malignant (Table S2). There were statistically significant differences in sex and age between the patients with benign and malignant nodules (P< 0.05) (Table S3). However, there were no significant differences in FT3, FT4, TSH, T3, and T4 values between the two groups.

Among the sonographic characteristics, malignant tumors had a higher A/T ratio than benign lesions (0.85±0.31 vs. 0.65±0.18, P=0.000) and were more likely to have markedly irregular morphology (52.33% vs. 16.37%, P=0.000), unclear margins (56.51% vs. 11.70%, P=0.000), and coexisting multiple microcalcifications (49.07% vs. 16.96%, P=0.000). The other characteristics of thyroid nodules, including tumor size, boundary, echogenicity, posterior echo attenuation, side shadowing, and blood flow, were significantly different between benign and malignant nodules (P< 0.05) (Table S3).

Multiple logistic regression analysis showed that the A/T ratio, multiple microcalcifications, and age were also associated with malignancy in the validation dataset. The A/T ratio had a significant and positive relationship with the risk of thyroid malignancy (OR 25.285, 95% CI 1.559-410.054) (Table 1). Younger age (OR 0.932, 95% CI 0.910-0.955) and the coexistence of multiple microcalcifications (OR 2.976, 95% CI 1.118-7.924) were independently associated with an increased risk for malignant nodules. The other parameters related to malignancy are shown in Table S5.

4.3. Diagnostic Performance of the Random Forest Model

A total of 53 US features and clinical features were used to build the models. The random forest model was trained on the training dataset with 1218 lesions and validated on an independent test dataset of 601 lesions. The top five weighted features, including the A/T ratio, margin, age, morphology, and multiple microcalcifications, were obtained from feature selection (Figure 1).

After 5-fold cross-validation in the training dataset, the AUC including the A/T ratio was 0.897, which was significantly higher than that without the A/T ratio (AUC: 0.862) (P<0.05). The AUC including the A/T ratio in the validation dataset was 0.769, which was also significantly higher than that without the A/T ratio (AUC: 0.716) (P<0.05) (Table 2) (Figure 1). The calibration curve demonstrated good agreement between the predictions and diagnoses of malignancy in the training dataset. The Hosmer-Lemeshow test result showed no departure from a perfect fit. The decision curves in the validation dataset showed that if the threshold probability was between 0.3 and 1.0 or more than 0.06, it was beneficial to use the model to predict malignancy (Table 2).

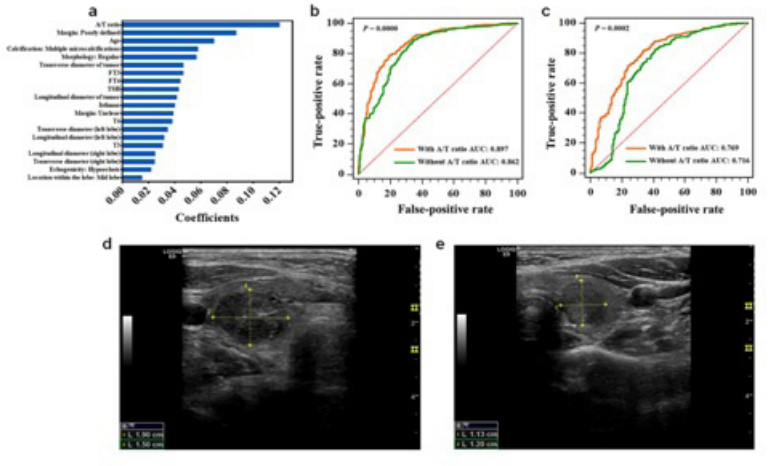

Figure 1: The predictive performance of the random forest model and US images of the thyroid. (a) The weighted features of the random forest model. (b) The AUC of the random forest model with and without the A/T ratio for predicting malignancy in the training dataset. (c) The AUC of the random forest model with and without the A/T ratio or predicting malignancy in the validation dataset. (d) A 52-year-old female with a 19.0×15.0 mm thyroid nodule with a regular shape, clear margin, and multiple calcifications that was pathologically diagnosed as a benign nodule. (e) A 35-year-old female with an 11.3×12.0 mm thyroid nodule with an irregular shape, unclear margin, A/T>1, and no calcification that was pathologically diagnosed as malignant.

Table 2: The diagnostic performance of the random forest and nomogram models in the training and validation datasets

		Accuracy	Sensitivity	Specificity	PPV	NPV	AUC [95% CI]
Random forest model	Training dataset	87.44%	95.59%	61.11%	88.81%	81.11%	0.897 (0.875-0.919)**
	Training dataset without A/T ratio	80.38%	81.40%	77.08%	91.98%	56.20%	0.862 (0.845-0.884)**
	Validation dataset	74.88%	80.00%	61.99%	84.11%	55.21%	0.769 (0.725-0.812)*
	Validation dataset without A/T ratio	44.49%	28.84%	82.46%	80.52%	31.54%	0.716 (0.664-0.769)*
Nomogram model	Training dataset	70.61%	66.56%	83.68%	92.94%	43.66%	0.823 (0.795-0.850)**
	Training dataset without A/T ratio	71.02%	73.87%	61.81%	86.20%	42.28%	0.728 (0.702-0.753**
	Validation dataset	76.04%	76.74%	74.27%	88.24%	55.95%	0.818 (0.779-0.856)**
	Validation dataset without A/T ratio	71.71%	96.75%	82.40%	72.77%	50.00%	0.732 (0.694-0.767)**
A/T cutoff point = 0.900 (proposed)	Training dataset	42.20%	25.81%	95.14%	94.49%	28.42%	0.735 (0.703-0.767)
	Validation dataset	78.37%	74.81%	85.29%	90.83%	63.50%	0.745 (0.702-0.787)

PPV: positive predictive value; NPV: negative predictive value; AUC: area under the curve; CI: confidence interval. **P< 0.0001; * P< 0.01.

4.4. Diagnostic Performance of the Nomogram Model

Multiple logistic regression analysis identified three factors, including age, A/T ratio, and multiple microcalcifications that were significantly related to malignancy. Furthermore, those factors were also highly weighted in the random forest model in the training dataset. These features were applied to develop the nomogram in the training dataset, and the nomogram was tested in the validation dataset. The nomogram showed high discrimination between benign and malignant lesions with an AUC of 0.823 (95% CI: 0.795-0.850) in the training dataset and an AUC of 0.818 (95% CI: 0.779-0.856) in the validation dataset, which was also significantly higher than that without the A/T ratio in the models (training dataset AUC: 0.728, validation dataset AUC: 0.732, all P<0.05) (Figure 2).

4.5. The Diagnostic Performance of the A/T Ratio

Since the A/T ratio played the most important role in our study, we plotted the ROC curves of the A/T ratio alone to assess diagnostic performance. The AUC of the A/T ratio in the training dataset was 0.735 (95% CI: 0.703-0.767). With a specificity of nearly 95% for diagnosing malignancy, the cutoff value in the training dataset was 0.900 (Table 1) (Figure 3). When using the A/T ratio of 0.900 as the cutoff value in the validation dataset, the AUC was 0.745 (95% CI: 0.702-0.787), with a sensitivity and specificity of 74.81% and 85.29%, respectively (Table 2).

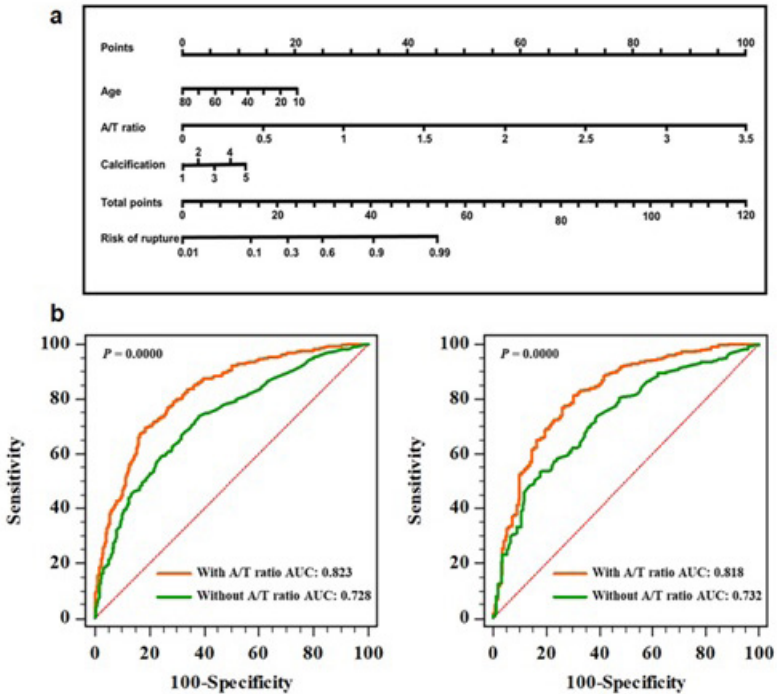

Figure 2: The nomogram and its diagnostic performance. (a) The nomogram was developed in the training dataset. It included three factors (A/T ratio, age, and calcifications). The nomogram plot provides a visual way to predict the risk of malignancy. Calcification: 1: None of the calcifications; 2: a microcalcification; 3: multiple microcalcifications; 4: cluster of microcalcifications; 5: coarse calcifications. (b) The ROC curve of the nomogram with and without the A/T ratio for predicting malignancy in the training dataset. (c) The ROC curve of the nomogram with and without the A/T ratio for predicting malignancy in the validation dataset

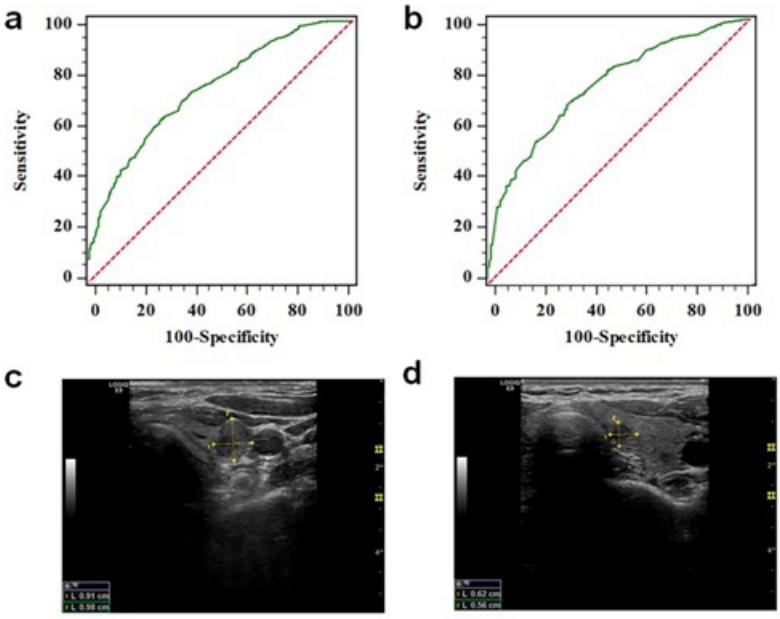

Figure 3: The ROC curves of the A/T ratio. (a) The ROC curves of the A/T ratio in the training dataset. (b) The ROC curves of the A/T ratio in the validation dataset. (c) Thyroid nodule with an A/T ratio = 1.077 that was diagnosed as malignant. (d) Thyroid nodule with an A/T ratio = 0.903 that was also diagnosed as malignant.

5. Discussion

In the present study, we developed and internally validated a clinical model and a nomogram model based on US features to estimate the risk of malignancy and thereby facilitate the management of patients with thyroid nodules. We found that the clinical model including A/T ratio had an AUC of 0.897 in the training dataset and an AUC of 0.769 in the validation dataset in random forest model, and had an AUC of 0.823 in the training dataset and an AUC of 0.818 in the validation dataset in nomogram models for diagnosing malignant nodules, which were significantly higher than those of without A/T ratio. Notably, we identified that the A/T ratio makes the largest contribution to the clinical and nomogram model, playing the most important role as an independent risk predictor. As a single predictive factor, A/T = 0.9 had a high specificity of 95% in the diagnosis of malignancy in the training dataset, which yielded a high sensitivity of 74.81% and a high specificity of 85.29% when applied to the validation dataset. This strong association with malignancy exists irrespective of other characteristics and might reduce the misdiagnosis in ruling out benign nodules and, in particular, pinpointing nodules for which fine-needle biopsy can safely be performed.

Clinical models are important in creating lesion-tailored work-ups and optimizing the management of resources. Multiple studies have shown that the features in clinical models of thyroid nodules are closely related to benignity and malignancy and can provide solid evidence for diagnosis [30-32]. However, few have taken full advantage of assessing the likelihood of malignancy due to the heterogeneity and small number of patients. In our study, we included 1218 lesions and convincingly found that multiple features, including the A/T ratio, calcifications, and age, were crucial for diagnosis. These results were also validated using 601 lesions from outside hospitals. The AUCs in the training and validation datasets were 0.897 and 0.769, respectively, which were higher than those previously reported [25, 33], further confirming the advantages and stability of this clinical model.

In our study, the clinical model showed that age, nodules with an A/T ratio larger than 0.9 and microcalcifications were the most important factors predicting malignancy in multivariate regression analysis. The A/T ratio had a much higher OR than age and microcalcifications for malignancy (41.833 vs. 0.961 vs. 4.618). Consequently, when adding the A/T ratio to evaluate the diagnostic accuracy, the AUCs significantly increased in the random forest models and nomogram models, demonstrating the relatively good accuracy of an A/T ratio ≥ 0.9 alone in predicting malignancy. However, the results of multiple studies suggest that no individual US feature can accurately discriminate a malignant nodule, and US alone cannot be used for the decision of surgical intervention [10, 34, 35], and the coexistence of two or more highly suspicious US criteria greatly increases the potential risk for nodules being malignant [10, 36]. In our cases, the combination of age, microcalcifications and A/T ratio≥0.9 was an independent predictor of malignancy, and although the sensitivity was low, the specificity was 95%. This means that younger patients with the coexistence of microcalcifications in A/T ratio≥0.9 nodules provide strong evidence of malignancy. This reduction in the A/T ratio from a threshold of 1 to diagnose malignancy would increase the positive rate of risk stratification systems in ruling out benign nodules.

The mechanism by which malignant thyroid nodules with higher

A/T ratio grow across normal tissue planes has not been defined. However, a recent study speculated that an A/T ratio ≥1 in malignant thyroid nodules and an A/T ratio <1 in benign nodules are related to probe compression of the thyroid nodule during US examination [14]. The majority of benign nodules are composed of cystic components, leading to softer elasticity and less infiltration into the surrounding tissue, while dense fibrosis is seen in 56%–89% of papillary thyroid carcinomas [37-39], which may be the main cause of decreased compressibility Therefore, an A/T ratio ≥1 appears to be shown during the US examination of malignant nodules. In our study, all the malignant nodules were papillary thyroid carcinomas, and majority of them with an A/T ratio≥0.9 on US image. It can be explained by the malignant nodules smaller than 3 cm were included, which might compose of less dense fibrosis since the shorter course of the nodules when compared with those larger than 3 cm. However, these tests have limited effectiveness in large samples. Therefore, more data is needed to train the model.

This study had some limitations that should be noted. First, the evaluation of samples was retrospective, and only tumors measuring less than 3 cm were included. There was inevitable selection bias and limited clinical applicability. Second, although this study had a relatively large patient population, further investigations with larger patient populations are necessary to validate the diagnostic capabilities of the findings. Finally, all the US features of thyroid nodules were determined by a radiologist instead of radiomic features extracted from images in this study. We will investigate US radiomic analysis in future research.

6. Conclusion

In conclusion, this predictive model for malignancy based on a combination of clinical and sonographic features has good performance for distinguishing between benign and malignant thyroid lesions. An A/T ratio ≥0.9 can reduce misdiagnosis and contribute more to the predictive performance. These findings could improve the management of thyroid nodules by supporting clinicians and reducing the number of invasive surgical procedures for patients with low-risk thyroid nodules as well as help in clinical decision making.

References

1. Jameson JL. Minimizing unnecessary surgery for thyroid nodules, N Engl J Med. 2012; 367: 765-7.
2. Vaccarella S, Franceschi S, Bray F, Wild CP, Plummer M, Dal Maso L. Worldwide Thyroid-Cancer Epidemic? The Increasing Impact of Overdiagnosis, N Engl J Med. 2016; 375: 614-7.
3. Kwak JY, Han KH, Yoon JH, Moon HJ, Son EJ, Park SH, et al. Thyroid imaging reporting and data system for US features of nodules: a step in establishing better stratification of cancer risk, Radiology. 2011; 260: 892-9.
4. Haugen BR, Alexander EK, Bible KC, Doherty GM, Mandel SJ, Nikiforov YE, et al. 2015 American Thyroid Association Management Guidelines for Adult Patients with Thyroid Nodules and Differentiated Thyroid Cancer: The American Thyroid Association Guidelines Task Force on Thyroid Nodules and Differentiated Thyroid Cancer, Thyroid: official journal of the American Thyroid Association. 2016; 26: 1-133.
5. Tessler FN, Middleton WD, Grant EG, Hoang JK, Berland LL, Teefey SA, et al. ACR Thyroid Imaging, Reporting and Data System (TI-RADS): White Paper of the ACR TI-RADS Committee, J Am Coll Radiol. 2017; 14: 587-95.
6. Iannuccilli JD, Cronan JJ, Monchik JM. Risk for malignancy of thyroid nodules as assessed by sonographic criteria: the need for biopsy, J Ultrasound Med. 2004; 23: 1455-64.
7. Moon WJ, Jung SL, Lee JH, Na DG, Baek JH, Lee YH, et al. Thyroid Study Group, Head, R. Neck, Benign and malignant thyroid nodules: US differentiation--multicenter retrospective study, Radiology. 2008; 247: 762-70.
8. Moon HJ, Kwak JY, Kim EK, Kim MJ. A taller-than-wide shape in thyroid nodules in transverse and longitudinal ultrasonographic planes and the prediction of malignancy, Thyroid. 2011; 21: 1249-53.
9. Hamour AF, Yang W, Lee JJW, Wu V, Ziai H, Singh P, et al. Association of the Implementation of a Standardized Thyroid Ultrasonography Reporting Program With Documentation of Nodule Characteristics, JAMA Otolaryngol Head Neck Surg. 2021; 147: 343-9.
10. Cappelli C, Castellano M, Pirola I, Gandossi E, De Martino E, Cumetti D, et al. Thyroid nodule shape suggests malignancy, Eur J Endocrinol. 2006; 155: 27-31.
11. Papapostolou KD, Evangelopoulou CC, Ioannidis IA, Kassi GN, Morfas KS, Karaminas NI, et al. Taller-than-wide Thyroid Nodules With Microcalcifications Are at High Risk of Malignancy, In Vivo. 2020; 34: 2101-5.
12. Kim EK, Park CS, Chung WY, Oh KK, Kim DI, Lee JT, et al. New sonographic criteria for recommending fine-needle aspiration biopsy of nonpalpable solid nodules of the thyroid, AJR Am J Roentgenol. 2002; 178: 687-91.
13. Kim JY, Lee CH, Kim SY, Jeon WK, Kang JH, An SK, et al. Radiologic and pathologic findings of nonpalpable thyroid carcinomas detected by ultrasonography in a medical screening center, J Ultrasound Med. 2008; 27: 215-23.
14. Yoon SJ, Yoon DY, Chang SK, Seo YL, Yun EJ, Choi CS, et al. "Taller-than-wide sign" of thyroid malignancy: comparison between ultrasound and CT, AJR Am J Roentgenol. 2010; 194: W420-4.
15. Grani G, Lamartina L, Ramundo V, Falcone R, Lomonaco C, Ciotti L, M et al. Taller-Than-Wide Shape: A New Definition Improves the Specificity of TIRADS Systems, Eur Thyroid J. 2020; 9: 85-91.
16. Wu MH, Chen KY, Chen A, Chen CN. Software-Based Analysis of the Taller-Than-Wide Feature of High-Risk Thyroid Nodules, Ann Surg Oncol. 2021.
17. Cappelli C, Pirola I, Cumetti D, Micheletti L, Tironi A, Gandossi E, et al. Is the anteroposterior and transverse diameter ratio of non-

palpable thyroid nodules a sonographic criteria for recommending fine-needle aspiration cytology?, Clin Endocrinol (Oxf). 2005; 63: 689-93.

18. Campanella P, Ianni F, Rota CA, Corsello SM, Pontecorvi A. Quantification of cancer risk of each clinical and ultrasonographic suspicious feature of thyroid nodules: a systematic review and meta-analysis, Eur J Endocrinol. 2014; 170: R203-11.
19. Mattingly AS, Noel JE, Orloff LA. A Closer Look at "Taller-Than-Wide" Thyroid Nodules: Examining Dimension Ratio to Predict Malignancy, Otolaryngol Head Neck Surg. 2021; 1945998211051310.
20. Ren J, Liu B, Zhang LL, Li HY, Zhang F, Li S, et al. A taller-than-wide shape is a good predictor of papillary thyroid carcinoma in small solid nodules, J Ultrasound Med. 2015; 34: 19-26.
21. Smayra T, Charara Z, Sleilaty C, Boustany G, Menassa-Moussa L, Halaby G. Classification and Regression Tree (CART) model of sonographic signs in predicting thyroid nodules malignancy, Eur J Radiol Open. 2019; 6: 343-9.
22. Fang D, Ma W, Xu L, Liu Y, Ma X, Lu H. A Predictive Model to Distinguish Papillary Thyroid Carcinomas from Benign Thyroid Nodules Using Ultrasonographic Features: A Single-Center, Retrospective Analysis, Med Sci Monit. 2019; 25: 9409-15.
23. Zhu YC, AlZoubi A, Jassim S, Jiang Q, Zhang Q, Wang YB, et al. A generic deep learning framework to classify thyroid and breast lesions in ultrasound images, Ultrasonics. 2021; 110: 106300.
24. Wu GG, Lv WZ, Yin R, Xu JW, Yan YJ, Chen RX, et al. Deep Learning Based on ACR TI-RADS Can Improve the Differential Diagnosis of Thyroid Nodules, Front Oncol. 2021; 11: 575166.
25. Liu J, Zheng D, Li Q, Tang X, Luo Z, Yuan Z, et al. A predictive model of thyroid malignancy using clinical, biochemical and sonographic parameters for patients in a multi-center setting, BMC Endocr Disord. 2018; 18: 17.
26. Jin Z, Zhu Y, Zhang S, Xie F, Zhang M, Zhang Y, et al. Ultrasound Computer-Aided Diagnosis (CAD) Based on the Thyroid Imaging Reporting and Data System (TI-RADS) to Distinguish Benign from Malignant Thyroid Nodules and the Diagnostic Performance of Radiologists with Different Diagnostic Experience, Med Sci Monit. 2020; 26: e918452.
27. Chang Y, Paul AK, Kim N, Baek JH, Choi YJ, Ha EJ, et al. Computer-aided diagnosis for classifying benign versus malignant thyroid nodules based on ultrasound images: A comparison with radiologist-based assessments, Med Phys. 2016; 43: 554.
28. Sun C, Zhang Y, Chang Q, Liu T, Zhang S, Wang X, et al. Evaluation of a deep learning-based computer-aided diagnosis system for distinguishing benign from malignant thyroid nodules in ultrasound images, Med Phys. 2020; 47: 3952-60.
29. American Institute of Ultrasound in M. AIUM Practice Guideline for the performance of thyroid and parathyroid ultrasound examination, J Ultrasound Med. 2003; 22: 1126-30.
30. Akkus Z, Cai J, Boonrod A, Zeinoddini A, Weston AD, Philbrick KA, et al. A Survey of Deep-Learning Applications in Ultrasound: Artificial Intelligence-Powered Ultrasound for Improving Clinical Workflow, J Am Coll Radiol. 2019; 16: P1318-28.
31. Bai Z, Chang L, Yu R, Li X, Wei X, Yu M, et al. Thyroid nodules risk stratification through deep learning based on ultrasound images, Med Phys. 2020; 47: 6355-65.
32. Wei X, Zhu J, Zhang H, Gao H, Yu R, Liu Z, et al. Visual Interpretability in Computer-Assisted Diagnosis of Thyroid Nodules Using Ultrasound Images, Med Sci Monit. 2020; 26: e927007.
33. Witczak J, Taylor P, Chai J, Amphlett B, Soukias JM, Das G, et al. Predicting malignancy in thyroid nodules: feasibility of a predictive model integrating clinical, biochemical, and ultrasound characteristics, Thyroid Res. 2016; 9: 4.
34. Na DG, Baek JH, Sung JY, Kim JH, Kim JK, Choi YJ, et al. Thyroid Imaging Reporting and Data System Risk Stratification of Thyroid Nodules: Categorization Based on Solidity and Echogenicity, Thyroid : official journal of the American Thyroid Association. 2016; 26: 562-72.
35. Eun NL, Yoo MR, Gweon HM, Park AY, Kim JA, Youk JH, et al. Thyroid nodules with nondiagnostic results on repeat fine-needle aspiration biopsy: which nodules should be considered for repeat biopsy or surgery rather than follow-up?, Ultrasonography. 2016; 35: 234-43.
36. Papini E, Guglielmi R, Bianchini A, Crescenzi A, Taccogna S, Nardi F, et al. Risk of malignancy in nonpalpable thyroid nodules: predictive value of ultrasound and color-Doppler features, The Journal of clinical endocrinology and metabolism. 2002; 87: 1941-6.
37. Carcangiu ML, Zampi G, Rosai J. Papillary thyroid carcinoma: a study of its many morphologic expressions and clinical correlates. Pathol Annu. 1985; 20: 1-44.
38. Isarangkul W. Dense fibrosis. Another diagnostic criterion for papillary thyroid carcinoma, Arch Pathol Lab Med. 1993; 117: 645-6.
39. Vickery AL Jr. Thyroid papillary carcinoma. Pathological and philosophical controversies, Am J Surg Pathol. 1983; 7: 797-807.